Journal of Alzheimer's Disease 48 (2015) 1083–1094
DOI 10.3233/JAD-150327
IOS Press

AβPP-Transgenic 2576 Mice Mimic Cell Type-Specific Aspects of Acetyl-CoA-Linked Metabolic Deficits in Alzheimer's Disease

Hanna Bielarczyk[a], Agnieszka Jankowska-Kulawy[a], Corinna Höfling[b], Anna Ronowska[a], Sylwia Gul-Hinc[a], Steffen Roßner[b], Reinhard Schliebs[b], Tadeusz Pawelczyk[c] and Andrzej Szutowicz[a,*]
[a]*Department of Laboratory Medicine, Medical University of Gdańsk, Gdańsk, Poland*
[b]*Paul Flechsig Institute for Brain Research, University of Leipzig, Leipzig, Germany*
[c]*Department of Molecular Medicine, Medical University of Gdańsk, Gdańsk, Poland*

Accepted 22 July 2015

Abstract. The pyruvate-derived acetyl-CoA is a principal direct precursor substrate for bulk energy synthesis in the brain. Deficits of pyruvate dehydrogenase in the neocortex are common features of Alzheimer's disease and other age-related encephalopathies in humans. Therefore, amyloid-β overload in brains of diverse transgenic Alzheimer's disease model animals was investigated as one of neurotoxic compounds responsible for pyruvate dehydrogenase inhibition yielding deficits of cholinergic neurotransmission and cognitive functions. Brains of aged, 14–16-month-old Tg2576 mice contained 0.6 μmol/kg levels of amyloid-β_{1-42}. Activities of pyruvate dehydrogenase complex, choline acetyltransferase, and several enzymes of acetyl-CoA and energy metabolism were found to be unchanged in both forebrain mitochondria and synaptosomes of Tg2576 mice, indicating preservation of structural integrity at least in cholinergic neuronal cells. However, in transgenic brain synaptosomes, pyruvate utilization, mitochondrial levels, and cytoplasmic acetyl-CoA levels, as well as acetylcholine content and its quantal release, were all found to be decreased by 25–40%. On the contrary, activation of pyruvate utilization was detected and no alterations in acetyl-CoA content and citrate or α-ketoglutarate accumulation were observed in transgenic whole brain mitochondria. These data indicate that amyloid-β evoked deficits in acetyl-CoA are confined to mitochondrial and cytoplasmic compartments of Tg2576 nerve terminals, becoming early primary signals paving the path for further stages of neurodegeneration. On the other hand, acetyl-CoA synthesis in mitochondrial compartments of glial cells seems to be activated despite amyloid-β accumulated in transgenic brains.

Keywords: Acetylcholine, acetyl-CoA, amyloid-β, choline acetyltransferase, pyruvate dehydrogenase, synaptosomes, Tg2576 mice, whole brain mitochondria

INTRODUCTION

The accumulation of amyloid-β (Aβ) is considered to be both a morphological hallmark as well as an active cytotoxic factor in the pathomechanism of Alzheimer's disease (AD). Several clinical observations revealed accumulation of Aβ aggregates in AD prone regions of the brain, in both inherited and sporadic forms of this pathology [1, 2]. These alterations are accompanied by the loss of cholinergic innervation in cortical areas responsible for memory formation and other cognitive functions. Significant direct correlations have been found between impairments in cognitive/memory tests before patients' death and deficits of cholinergic markers such as choline acetyltrasferase (ChAT), muscarinic M_2 receptors, or vesicular acetylcholine transporter levels in selected hippocampal and cortical areas of autopsy brains [3, 4]. On the other hand, in elderly people in stages of mild cognitive impairment, Aβ overload in their brains was not accompanied by altered or even increased activities of ChAT [2, 5].

*Correspondence to: Andrzej Szutowicz, Department of Laboratory Medicine, Medical University of Gdańsk, Dębinki 7 str., Bldg. 27, 80-211 Gdańsk, Poland. Tel.: +48 583 492 770; Fax: +48 583 492 784; E-mail: aszut@gumed.edu.pl.

ISSN 1387-2877/15/$35.00

Marked accumulation of Aβ was also reported in brains of both apparently non-demented elderly people and in brains of young *APP/PSEN* gene mutations carriers, decades before the onset of dementia [1]. Nevertheless, people with mild cognitive impairment and AD with Aβ overload displayed faster cognitive decline than those mentally impaired but without significant amyloidosis in their brains [6]. This led to the conclusion that Aβ accumulation may be the outcome but not the cause of neurodegeneration in AD [2].

Studies on transgenic animals also revealed that early intraneuronal accumulation of mono/oligomeric Aβ preceded extracellular deposition of its polymers and tau peptides [7, 8]. The former exerted several toxic metabolic effects in neuronal cytoplasmic and mitochondrial compartments [9, 10]. These findings indicate that combinations of diverse pathologic signals may accompany and contribute to neurodegeneration by Aβ.

Another prominent feature of AD pathology is the impairment of brain energy metabolism. Functional PET studies of AD patient brains revealed significant inhibition of F^{18} deoxyglucose uptake as well as the decreases in their phosphocreatine/ATP or NAA levels [11, 12].

Among enzymes susceptible to these conditions are pyruvate and α-ketoglutarate dehydrogenase complexes (PDHC and KDHC), which are responsible for provision of acetyl-CoA and controlling the rate of metabolic flux through TCA cycle, respectively. Suppression of PDHC activity yielded shortages of acetyl-CoA in mitochondrial and cytoplasmic compartments in both rat brain nerve terminals and in cholinergic neuroblastoma cells [13]. In fact, decreases in mitochondrial acetyl-CoA, evoked by various neurodegenerative inputs, displayed significant inverse correlations with fractional contents of nonviable cells and their PDHC activity [13, 14]. On the other hand, suppression of acetyl-CoA formation in the cytoplasmic compartment of cholinergic neurons was found to correlate with inhibition of choline acetyltransferase activity, acetylcholine synthesis/level, and its quantal release [13, 14]. These *in vitro* findings appeared to be compatible with clinical and postmortem observations of AD brains. Studies of autopsied AD brains revealed suppressions of PDHC, KDHC, several other enzymes of tricarboxylic acid cycle, as well as respiratory chain in pathologically altered cortical areas [11, 15]. These enzymological alterations constitute the structural basis for apparent depression of energy metabolism in AD brains. Moreover, deficits in PDHC and energy metabolism were found to correlate significantly both with reductions in ChAT and other cholinergic markers as well as with impairments of cognitive functions shortly before death of AD patients [3, 11, 13, 16].

A number of transgenic mouse strains were used to study temporal and quantitative correlations between Aβ load and behavioral or metabolic alterations taking place in their brains [17]. Their genomes contained different combinations of single and multiple inserts of mutated human *APP/PS1* genes. There are, however, several-fold quantitative and temporal differences in accumulation pathogenic $A\beta_{1\text{-}42}$ peptides in brains of various transgenic AD mouse strains [18]. They were reported to range from 0.2 to over 10.0 μmol/kg of wet brain tissue [8, 19]. There is, however, no explanation why, despite of these differences, all strains displayed similar degree of age-dependent impairment of various behavioral/cognitive functions [17]. In different strains of AD-Tg mice, no losses in cholinergic protein markers were observed despite evident memory and cholinergic neurotransmission deficits [17, 20, 21]. Also, no depression in enzymes of respiratory chain and any consistent alterations in nerve terminal bioenergetics were observed in AD-Tg mice [20, 22]. On the contrary, in 3 × Tg-AD mice, the age-dependent depression of brain PDHC-E1 subunit level was found to be more evident than in non-Tg siblings [23]. For obvious reasons, there is lack of any data comparing activities of TCA cycle enzymes with acetyl-CoA metabolism in AD human brains [11, 15]. The former ones have been found to play a key role in early disturbances in cholinergic transmission, and neuronal survival in cellular models of AD pathology [13, 24]. Therefore, the aim of this study was to investigate whether increased Aβ load in brains of Tg2576 mice may be accompanied by appropriate alterations in acetyl-CoA energy and acetylcholine-transmitter metabolism.

MATERIALS AND METHODS

Reagents

Unless otherwise specified, biochemicals were obtained from Sigma-Aldrich (Poznań, Poland) and [1-^{14}C-acetyl]-CoA 4 mCi/mmol was from Perkin-Elmer (Boston, MA, USA).

Animals

The experiment was performed using 14–16 months old female and male Tg2576 hemizygous mice, containing the human *APP695* gene with double

K670N/M671L mutation (Tg2576), and their transgene negative siblings (WT). They were chosen as animal experimental model for this study because they develop an Aβ pathology that follows the temporal and spatial appearance comparable to that observed in AD patients. Moreover, these mice display age-dependent deficits in spatial learning in defined memory tasks. Since this mouse strain was used by numerous groups in the past two decades, a substantial amount of data accumulated that allows to compare some results of the current study with the literature [8, 17, 18, 21, 22]. They were obtained from K. Hsiao and maintained at the Leipzig University animal housing facility (Medizinisch Experimentelles Zentrum). Animals were housed in sex-selected groups of 4–6 per cage at constant temperature ($22 \pm 1^{\circ}$C) with 12 h/12h light/dark cycle, and free access to food and water. A total number of 25 Tg and 24 WT mice were tested (Ethical Commission on Animal Experiments permit to H. Bielarczyk No 8/2010GUMedWL, and T06/15 of the Regierungspräsidium Leipzig). They were sacrificed by decapitation and forebrains were taken either for immunohistochemistry, Aβ ELISA assays (6 Tg and 6 WT) or for isolation of synaptosomal (B) and whole brain mitochondrial (C) subfractions (19 Tg and 18 WT). Forebrains from 3 mice within each group were randomly combined to obtain sufficient amounts of subfractions for metabolic studies. They were isolated from 10% forebrain homogenates in 320 mM sucrose with 0.1 mmol/L EDTA, by the combination of differential and Ficoll-density gradient centrifugation, as described elsewhere [25]. Subfractions B and C were collected from ficoll density gradient and centrifugation-washed with 320 mmol/L sucrose containing 10 mmol/L NaHEPES pH 7.4 and 0.1 mmol/L EDTA [25]. Pellets were suspended in 320 mmol/L buffered sucrose and preparations were used for metabolic studies and enzyme assays.

Aβ immunohistochemistry

In order to prove the presence of Aβ deposits in brains of Tg mice, immunohistochemistry using the mouse-anti Aβ antibody 6E10 (Millipore, Germany) at a dilution of 1:2,000 was performed. After incubation with the primary antibody solution at 4°C overnight, brain sections of TG and WT mice were washed and incubated with secondary biotinylated donkey anti-mouse antibody (Dianova, Germany 1:400) followed by incubation with extravidin-conjugated peroxidase (Sigma-Aldrich, Germany; 1:2,000) in blocking solution for 60 min at room temperature. Finally, peroxidase binding was visualized with 2 mg DAB and 2.5 µl H_2O_2 per 5 ml Tris buffer (50 mmol/L; pH 7.6) resulting in a brown precipitate. The Aβ plaque load was calculated and is given as percent Aβ plaque coverage of the total brain volume.

Aβ ELISA assay

In order to quantify the Aβ load and aggregation state in brains of Tg2576 mice at the time of biochemical analyses, $A\beta_{1\text{-}40}$ and $A\beta_{1\text{-}42}$ concentrations were determined. Hippocampal and cortical brain tissue was homogenized in 2.5 ml Tris buffered saline (TBS), centrifuged at 40,000× *g* for 1 h at 4°C and the supernatants containing soluble Aβ (TBS fraction) were stored at –80°C pending analysis. The pellets were re-suspended in 2% sodium dodecyl sulfate (SDS), centrifuged at 40,000× *g* for 1 h at 4°C and the supernatants containing Aβ oligomers and pre-fibrils (SDS fraction) were stored at –80°C. The resultant pellets were finally re-suspended in 70% formic acid (FA) to solubilize Aβ fibrils. ELISAs were performed using $A\beta_{1\text{-}40}$ and $A\beta_{1\text{-}42}$ specific kits (IBL RE59751 and RE59731, Hamburg, Germany) following the manufacturers' instructions and the concentrations are given as nmol Aβ/kg brain tissue.

Metabolic studies of nerve terminals

The basic, depolarizing incubation medium contained in a final volume of 1.0 ml: 2.5 mM pyruvate, 2.5 mM L-malate, 90 mM NaCl, 30 mM KCl, 20 mM, 1.0 mM $CaCl_2$, NaHEPES (pH 7.4), 1.5 mM Na-phosphate, 0.01 mM choline chloride, 0.015 mM eserine sulfate, 32 mM sucrose, 1.2–1.5 mg of synaptosomal protein. The 30 mM K^+ and 1 mM Ca^{2+} were employed to induce depolarization-dependent steady maximal rates of ACh release and resynthesis during entire period of synaptosomes incubation [25, 26]. Incubation was started by the addition of synaptosome suspension and continued in an ambient atmosphere for 30 min at 37°C with shaking at 100 cycles per min. The appropriate volumes of synaptosome suspension were taken for assessment different metabolic parameters.

Metabolic studies of whole brain mitochondria

Basic incubation medium contained in a final volume of 1.0 mL: 2.5 mM pyruvate, 2.5 mmol/L L-malate, 50 mmol/L KCl, 20 mmol/L NaHEPES buffer (pH 7.4), 5 mmol/L KH_2PO_4/K_2HPO_4 buffer (pH 7.4), 0.01 mmol/L EDTA, 132 mmol/L sucrose.

Incubation was started by the addition of 0.1 mL (0.5 mg of protein) mitochondrial suspension and carried out for 15 min at 37°C with shaking at 100 cycles/min. At the end of incubation, 0.4 mL specimens of the mitochondrial suspension were deproteinized with 6% perchloric acid.

Clear acid extracts were neutralized with K_2CO_3 and used for pyruvate, citrate and α-ketoglutarate assays as described elsewhere [25]. Remaining part of the suspension was centrifuged for 40 s at 12,000× *g* in refrigerated centrifuge, and pellet deproteinized with 6% perchloric acid for acetyl-CoA assay (see below).

Pyruvate, lactate, citrate, and α-ketoglutarate assays

Samples of the incubation medium with suspended synaptosomes (0.4 mL) were deproteinized with 6% $HClO_4$ and after neutralization with K_2CO_3 were used for metabolite determinations by spectrophotometric methods described elsewhere [25]. The pyruvate utilization as well as, citrate and α-ketoglutarate accumulation was calculated from the difference between metabolite content in 30 min incubated sample and its content in specimen deproteinized at zero time.

Acetyl-CoA assay

For the determination of acetyl-CoA content in whole synaptosomes, 0.3 mL of synaptosomal suspension was centrifuged at 5,000× *g* for 1 min at +4°C. Resulting pellet was deproteinized by suspension in a small volume of 5 mmol/L HCl and incubation in a boiling bath for 1 min. To assess the acetyl-CoA content in synaptosomal mitochondria, 0.5 ml of incubation synaptosomal suspension was mixed with equal volume of ice cold lysing solution containing 1.4 mg digitonin/mL in 125 mmol/L KCl with 20 mM NaHEPES buffer (pH 7.4) and 3 mmol/L EDTA. Lysate was transferred on 0.5 mL of silicone oil mixture (AR 20 and AR200, 1:2) layered over 0.1 mL of buffered 320 mmol/L sucrose. After 30 s the mitochondrial fraction was separated from the soluble one by centrifugation for 40 s at 12,000× *g* in refrigerated centrifuge. After removal of the soluble fraction, silicon oils, and sucrose, the mitochondrial pellet was deproteinized as described above. Deproteinized extracts of whole synaptosomes and synaptosomal mitochondria were treated with maleic anhydride solution in ethyl ether for 2 h to remove free coenzyme A. Cycling reaction was carried for 60 min in 0.1 mL of the medium containing 1.9 mmol/L acetyl phosphate, 1.2 mmol/L oxaloacetate, 1.0 IU phosphotransacetylase, and 0.12 IU citrate synthase. Cycling reaction was stopped by heating samples at 100°C for 10 min and citrate formed was determined [27]. The level of cytoplasmic acetyl-CoA was calculated by subtraction of the mitochondrial acetyl-CoA content from the content of acetyl-CoA in whole synaptosomes [27].

Acetylcholine assay

Samples (0.2 mL) of synaptosomal suspension were centrifuged 3 min at 10,000× *g*. Supernatants were collected and used for determination of released acetylcholine (ACh) with acetylcholinesterase-choline oxidase, coupled with peroxidase–luminol detection system [28] using Junior luminometer (Berthold Technology, Bad Wild-Bad, Germany).

Enzyme assays

Immediately before the assay synaptosomal suspension was diluted to desired protein concentration with 0.2% v/v Triton X-100. ChAT activity was assessed by the radiometric method using [1-^{14}C]acetyl-CoA as a substrate [29]. The PDHC was assayed by the citrate synthase coupled method [30]. The KDHC activity was determined by a direct measurement of the NAD reduction [31]. Aconitase, NADP-isocitrate dehydrogenase and ATP-citrate lyase (acetyl-CoA:oxaloacetate *C*-acetyltransferase[(*pro-S*)carboxymethyl-forming, ADP phosphorylating, EC 2.3.3.8, ACL) were assayed by methods described elsewhere [32–34]. For studies of direct inhibition of mitochondrial enzymes, oligomerized forms of $A\beta_{25-35}$ and $A\beta_{1-42}$, were prepared, as described elsewhere [35].

Protein assay

Protein was assayed by the method of Bradford [36] with human immunoglobulin as a standard.

Statistics

Statistical analyses were carried out by non-paired Student's *t* test, at $p < 0.05$ being considered to be statistically significant using Prism 4.0 graphic-statistical program.

RESULTS

Characteristics of experimental groups

In brains of 16-month-old AβPP-transgenic Tg2576 mice, the plaque load quantified by analysis of

immunohistochemical labeling amounted to approximately 3%, whereas no Aβ deposits were detected in any of the WT control brains (Fig. 1A). The quantification of Aβ by ELISA revealed low concentrations of $A\beta_{1\text{-}40}$ and of $A\beta_{1\text{-}42}$ in the soluble TBS fraction being equal to 5.2 nmol/kg and 4.4 nmol/kg of wet brain tissue, respectively (Fig. 1B). A much higher abundance of both Aβ peptide variants was detected in the SDS and FA-extractable fractions. In each of these fractions, the $A\beta_{1\text{-}40}$ concentrations were several times higher than those of $A\beta_{1\text{-}42}$. Thus, in SDS fraction $A\beta_{1\text{-}40}$ levels were 3770 nmol/kg, and $A\beta_{1\text{-}42}$ 390 nmol/kg, respectively. In FA fraction: $A\beta_{1\text{-}40}$ level was equal to 1170 nmol/kg, and that of $A\beta_{1\text{-}42}$ 240 nmol/kg, respectively (Fig. 1B). No detectable amounts of Aβ were found in brains of WT siblings (Fig. 1A).

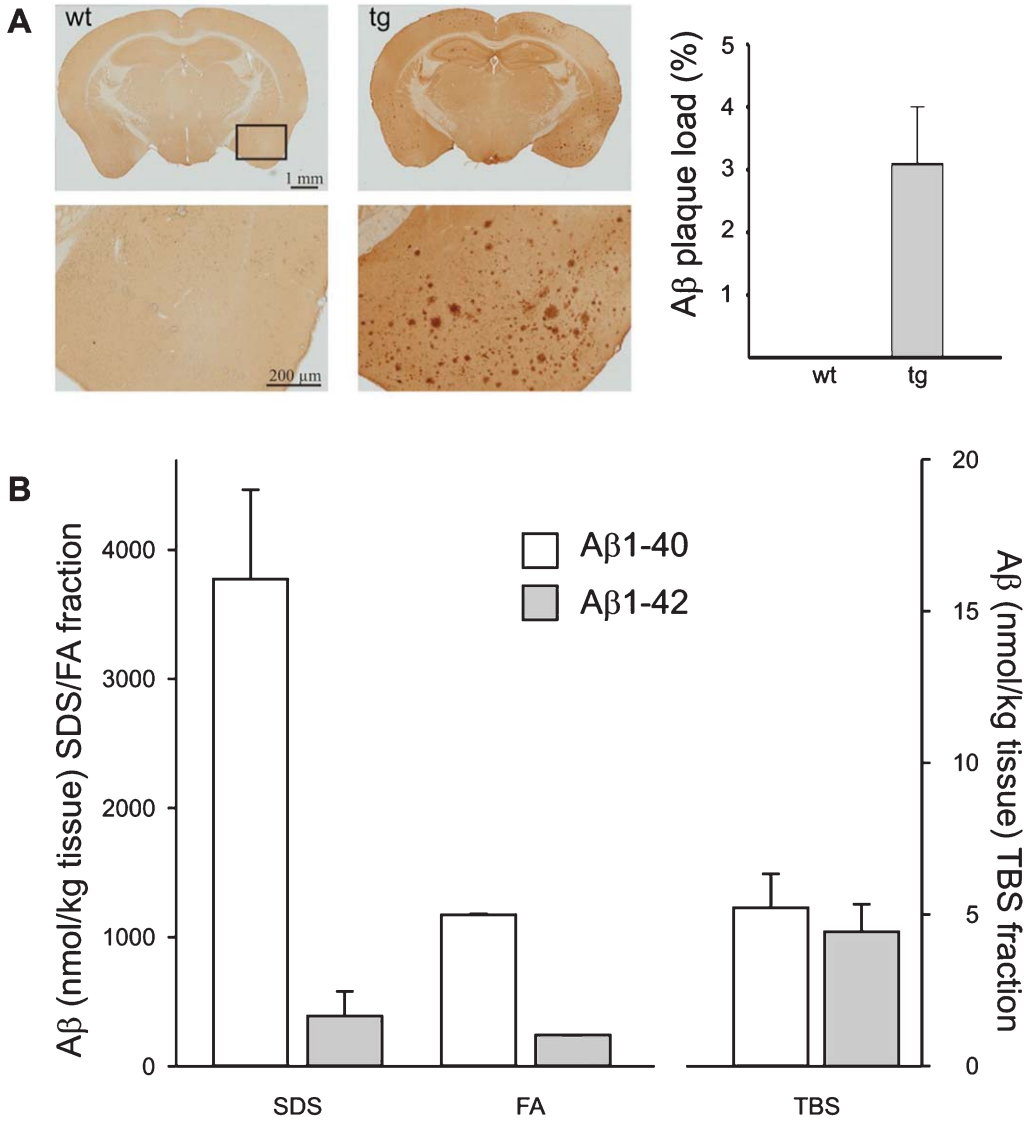

Fig. 1. Biochemical analyses of Aβ pathology in brains of 16 months old Tg2576 mice and age-matched WT littermates. A) Representative immunohistochemical staining and quantification of Aβ plaques with 6E10 and quantification of the plaque load in these mice ($n = 4$, each). B) Quantification of Aβ concentrations in brains of transgenic ($n = 6$) and wildtype mice ($n = 2$) by ELISA analysis. Soluble Aβ was solved in TBS followed by extractions Aβ of low solubility in SDS and formic acid (FA) fractions. Quantitative data are means ± SEM.

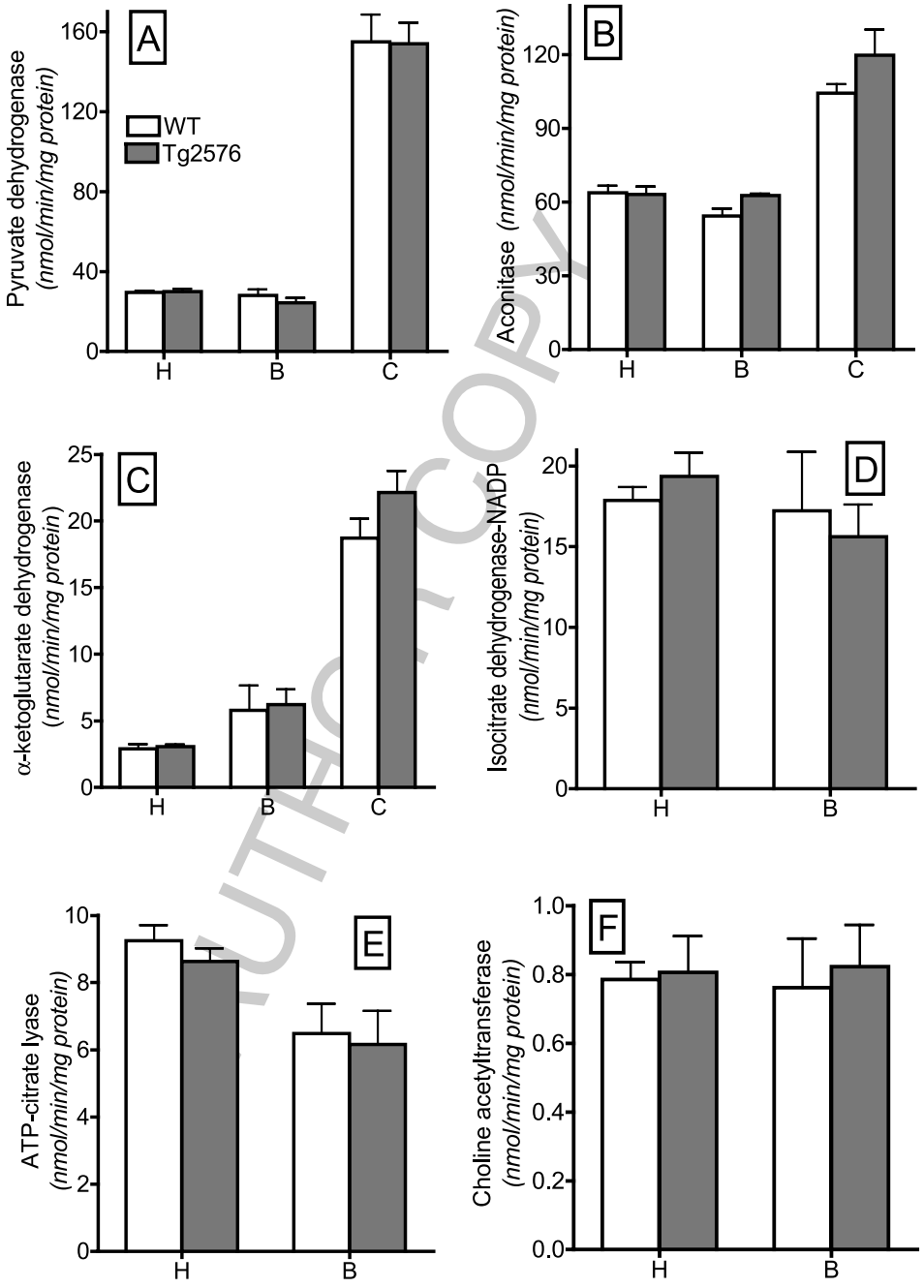

Fig. 2. Enzymes of energy and acetyl-CoA metabolism in homogenate (H), synaptosomal (B), and whole brain mitochondria (C) subfractions from forebrains of Tg2576 and WT mice. Data are means ± SEM from 4–6 experiments.

Enzyme activities

Fractionation of forebrain homogenates yielded whole brain mitochondrial sub-fraction C highly enriched in PDHC and KDHC activities. The relative specific activities of PDHC in sub-fraction C against homogenate were 5.2 and 5.1 for WT and Tg2576 groups, respectively (Fig. 2A). In the same sub-fractions relative specific activities for KDHC were equal to 6.4 and 7.2, respectively (Fig. 2C). No substantial enrichment of those enzymes was detected in synaptosomal sub-fractions B in both groups. Specific activities of enzymes of exclusive mitochondrial localization PDHC and KDHC, as well as those of

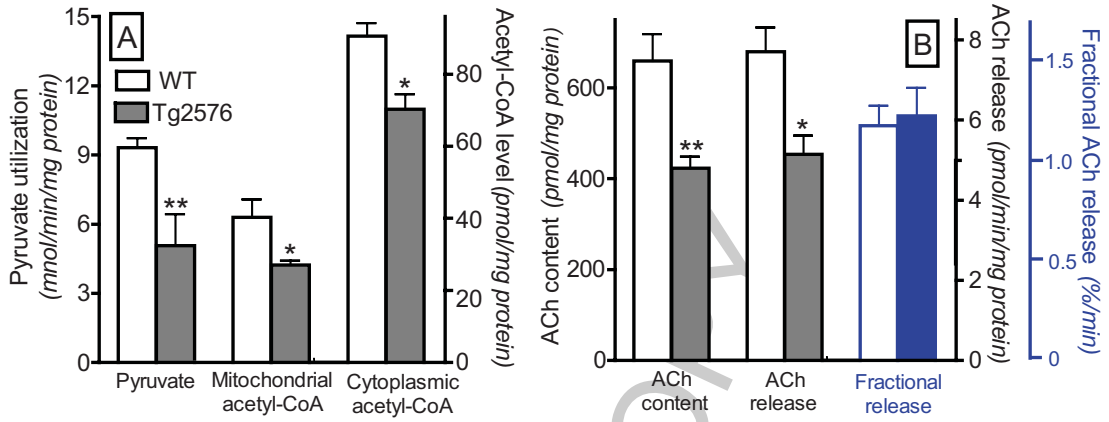

Fig. 3. Parameters of acetyl-CoA metabolism in synaptosomes from forebrains of Tg2576 and WT mice. A) Pyruvate utilization and mitochondrial acetyl-CoA level. B) Synaptoplasmic acetyl–CoA and synaptosomal acetylcholine levels. Data are means ± SEM from 4–6 experiments. Significantly different from respective WT values: $^{*}p < 0.01$, $^{**}p < 0.001$.

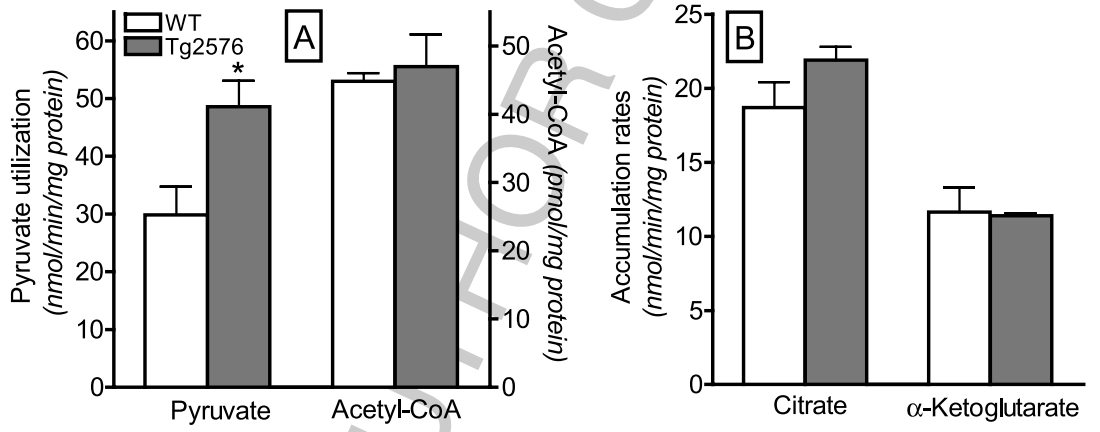

Fig. 4. Parameters of acetyl-CoA metabolism in whole brain mitochondria from forebrains of Tg2576 and WT mice. A) Pyruvate utilization and mitochondrial acetyl-CoA level. B) Citrate and α-ketoglutarate accumulation rates. Data are means ± SEM from 4–6 experiments. Significantly different from respective WT values: $^{*}p < 0.01$.

mixed mitochondrial-cytoplasmic localization, aconitase and isocitrate-NADP dehydrogenase, were found to be similar in WT and Tg2576 mice brain cortices homogenates and synaptosomal fractions (Fig. 2A-D). Activity of ATP-citrate lyase, cytoplasmic enzyme involved in indirect transport of acetyl units from mitochondria to cytoplasm was not altered in Tg2576 brains (Fig. 2E). Also activity of key marker enzyme of cholinergic neurons, choline acetyltransferase in homogenates and synaptosomes derived fromTg2576 brains, was not inhibited by accumulated Aβ (Fig. 2F).

Synaptosomal metabolism

Pyruvate utilization by Tg2576 synaptosomes was 46% lower than those from WT mice (Fig. 3A). Also the level of acetyl-CoA in Tg2576 synaptosomal mitochondria was decreased by 33% (Fig. 3A). Accordingly, levels of synaptoplasmic acetyl-CoA and synaptosomal acetylcholine were suppressed in aged Tg2576 in respect to WT, by 23 and 36%, respectively (Fig. 3A, B). The rate K^{+}/Ca^{2+} evoked ACh release from Tg2576 synaptosomes was 33% lower than that in the WT ones, the absolute value of which being equal to 7.70 ± 0.61 pmol/min/mg protein (Fig. 3B). On the contrary, calculated fractional rates of transmitter release from synaptosomes appeared to be same in both groups being equal to 1.22 and 1.17% of its whole pools in Tg2576 and WT nerve terminals, respectively (Fig. 3B).

Whole brain mitochondria metabolism

Pyruvate utilization in whole brain mitochondria of Tg2576 mice was 63% higher than that in WT mice

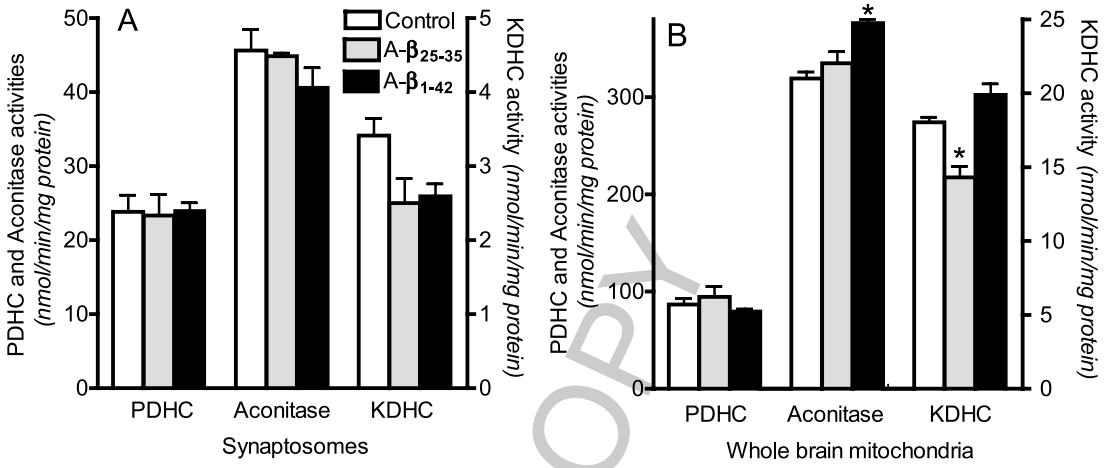

Fig. 5. Effects of 0.02 mmol/L concentration of A-β_{25-35} and A-β_{1-42} on activities of mitochondrial enzymes in lysates of: (A) synaptosomal and (B) whole brain mitochondrial factions data are means ± SEM from 4 experiments. Significantly different from respective controls $^{*}p < 0.01$.

(Fig. 4A). Despite that, acetyl-CoA levels, as well as citrate and α-ketoglutarate accumulation rates, in whole brain mitochondria appeared to be similar in both groups (Fig. 4A, B).

Direct effects of Aβ on PDHC and aconitase activities

Neither $A\beta_{25-35}$ nor $A\beta_{1-42}$ oligomers in high, pathologically non-relevant, 0.02 mmol/L concentrations exerted direct significant inhibitory effects on PDHC, aconitase, and KDHC activities neither in triton-X-100 solubilized synaptosomal nor in whole brain cortex mitochondrial fractions (Fig. 5). Lower (0.010 and 0.005 mmol/L) concentrations of $A\beta_{25-35}$ and $A\beta_{1-42}$ also did not alter activities of those enzymes (not shown).

DISCUSSION

The 14–16-month-old mice used here displayed relatively high level of overall $A\beta_{1-42}$ accumulation in their brain cortex (Fig. 1B). The sum of levels of all $A\beta_{1-42}$ subfractions equal to 630 nmol/kg appeared to be about 1.5–6.0 times higher than levels of guanidine or SDS-formic acid extractable $A\beta_{1-42}$, in brain cortices of somewhat younger AD-Tg mice of different strains (Fig. 1) [19, 37, 38]. This value is also comparable with overall $A\beta_{1-42}$ levels reported for different regions of human brain cortex affected by AD [2, 19, 39]. We have found that TBS-soluble monomers of $A\beta_{1-40}$ and $A\beta_{1-42}$ constitute only about 0.5–1% overall amyloid load in Tg2576 brains what remains in accord with reports quoted above (Fig. 1B) [40, 41]. Thus, 14–16-month-old Tg2576 mice, used here, constituted a decent model for studying putative mechanisms of disturbances in energy-acetyl-CoA metabolism apparently taking place in brain cortex of patients with both mild and severe cognitive deficits (Fig. 1B) [1, 2, 11, 39].

Our past data demonstrated that both exogenous $A\beta_{25-35}$ and $A\beta_{1-42}$ in submicromolar and micromolar concentrations exerted neurotoxic and cholino-suppressory effects on cultured cholinergic neuronal cells that correlated with deficits of mitochondrial enzymes and acetyl-CoA in their mitochondrial and cytoplasmic compartments, respectively [13, 14, 42, 43].

However, PDHC, aconitase, and KDHC in Tg2576 synaptosomal or mitochondrial homogenates appeared to be resistant to direct exposition to very high concentrations of both cytotoxic fragment $A\beta_{25-35}$ and $A\beta_{1-42}$ oligomers (Fig. 5). Also the activities of mitochondrial/cytoplasmic enzymes in solubilized Tg2576 synaptosomes or whole brain mitochondria were not found to be decreased (Fig. 2). These findings point out that the suppression of pyruvate-acetyl-CoA metabolism in the neuronal terminals was brought about by interactions of accumulated Aβ with other cell surface or other intracellular molecular targets, yielding indirect *in situ* inhibition of this enzyme (Figs. 1, 3A, 5) [44–46]. Such a conclusion is supported by the fact that synaptosomal mitochondria from TgAβPP mice contained high (about 5 μmol/L) levels of $A\beta_{1-42}$ [47]. Also, exogenous oligomeric $A\beta_{1-42}$ added to culture medium inhibited pyruvate

oxidation/PDHC activity both in cultured viable rat forebrain neurons and in cholinergic SN56 neuroblastoma cells [13, 42, 44].

The data presented here are compatible with clinical observations in humans carrying AD-associated mutations. They displayed decreases in glucose metabolism as well as increased Aβ accumulation in their brains preceding clinical onset of cognitive impairment and decay of cortical neurons (Figs. 1–3) [1].

On the other hand, inhibitory effects of Aβ, accumulated in brains of Tg2576 mice, on pyruvate utilization and acetyl-CoA level in isolated synaptosomes indicate the existence *in vivo* suppression its metabolic flux through the PDHC step (Fig. 3A). It could be evoked by Aβ-induced high increases in cytoplasmic $[Ca^{2+}]$ that might activate excessive synthesis of reactive oxygen species and nitrozyl radicals [48–50]. The former were found to suppress acetyl-CoA synthesis due to inhibition of PDHC and other enzymes of energy metabolism *in situ* in neuronal/synaptosomal mitochondria [42, 46, 51, 52].

Oxidative stress induced by Aβ was also found to oxidize lipoic acid, a cofactor of PDHC, thereby suppressing its activity *in situ* [53]. It would explain why exogenous lipoic acid overcame inhibitory effects of Aβ and NO excess on PDHC and KDHC and viability of cultured cholinergic SN56 cells and metabolic deficits in triple transgenic AD mice [42, 43, 54]. Another mechanism of Aβ suppressory effects may result from its activation of tau protein kinase I/glycogen synthase kinase 3β, that were found to inhibit PDHC in cultured hippocampal neurons, through the inhibitory phosphorylation of this enzyme [45].

Such conclusions are supported by the fact that inhibition of pyruvate utilization by Aβ was observed only in whole synaptosomes but not in synaptosomal lysates at optimal concentrations of substrates and co-factors (Figs. 2A, 3A, 5). Moreover, the presented data indicate that apparent amyloid-overload evoked suppressive effects were limited to the neuronal compartment, since no activation or alterations of pyruvate utilization or PDHC activity were observed in Tg2576 whole brain glial mitochondria (Figs. 2A, 4A). In addition, unchanged levels of acetyl-CoA and rates of citrate and α-ketoglutarate accumulation document preservation of acetyl-CoA to the α-ketoglutarate metabolic pathway in the mitochondrial compartment of glial cells in Tg2576, Aβ overloaded brain (Figs. 2B, C, 4A, B). Such differential patterns of PDHC activities *in situ* in subfractions B and C may result from the fact that in nonsynaptic transgenic mitochondria, no oxidative stress was present and accumulation of Aβ was over 3 times lower than in synaptic mitochondria (Figs. 3A, 4A) [47].

Aβ-evoked excitotoxic accumulation of Zn^{2+} and NOO^{-} radicals may bring about direct inhibition or inactivation of several enzymes of energy metabolism including PDHC, aconitase, and KDHC, yielding suppression of ACh metabolism (Fig. 3A, B) [47, 55, 56]. Thereby they became final executors of Aβ signals [42, 57–59]. Such PDHC *in situ* inhibition was revealed in cholinergic Zn-exposed SN56 cells, and could result from interactions of Zn^{2+} and peroxynitrite with its lipoamide binding sites (Fig. 3A) [13, 42, 47]. The likelihood of such mechanism is supported by finding of Zn dyshomeostasis in brains of Tg2576 mice [60].

On the other hand, if such conditions would prevail in Aβ-bearing Tg2576 brains, then decreases in PDHC and aconitase activities should be detected. That was, however, not the case (Figs. 1, 2). In this respect, Tg2576 brain does not resemble the condition of human AD brain, in which marked reductions in mitochondrial enzymes activities were observed (Fig. 2) [11]. Presumably coexistence of Aβ excess with multiple neurotoxic signals is required for full presentation of this feature of AD pathology [61]. Such claim is supported by the fact that 3 × Tg-AD female mice, carrying three mutated AD-related genes, displayed significant decreases in PDHC activities in their brain mitochondria [23].

Nevertheless, Aβ accumulated in Tg2576 brain was sufficient to evoke the indirect inhibition of the metabolic flux of pyruvate through PDHC step *in situ* in synaptosomal mitochondria (Figs. 1, 3A, 5) [44, 45]. Irrespective of the detailed mechanism, such *in situ* inhibition could be responsible for primary suppression of acetyl-CoA in the synaptosomal mitochondria (Fig. 3A). These shortages could attenuate direct acetyl-CoA transport through the mitochondrial membrane yielding secondary suppression of its level in synaptoplasm (Fig. 3B) [13, 26]. Decreased availability of acetyl-CoA in synaptoplasm could compromise ACh synthesis by ChAT, despite of not suppressed activity of this enzyme. It also resulted in the decrease of steady-state level of ACh in nerve terminals, as dependent on ChAT reaction equilibrium constant (Figs. 2F, 3B) [13, 26].

On the other hand, ATP-citrate lyase pathway of indirect transport of acetyl units from synaptosomal mitochondria to cytoplasm seems to be not affected in Tg2576, due to unchanged enzyme activity (Fig. 2E). Therefore, decreased content and rate of K^{+}-evoked ACh release in Tg nerve terminals resulted from

impediment of acetyl-CoA supply from mitochondria through direct PTP-dependent transport (Fig. 3A, B) [25]. However, the mechanisms of quantal ACh release itself were apparently not affected by amyloidosis, since values of fractional transmitter release in Tg2576 and WT groups were the same (Fig. 3B) [26]. The present findings complement earlier ones, which demonstrated no alterations in ChAT and acetylcholinesterase activities, but decreased densities of M1/M2 muscarinic and nicotinic receptors in brains of Tg2576 mice [37]. Also *in vivo* microdalysis studies revealed a decrease in scopolamine-induced ACh release, but not altered ChAT activities in brains of Tg2576 mice [21]. Similar effects were observed in cultured primary septal/forebrain neurons upon their exposition to nontoxic Aβ (0.1 μmol/L) concentrations, which inhibited PDHC activity and ACh synthesis without altering ChAT [44, 45].

These findings do not remain in line with autopsy studies of human AD brains, which revealed evident decreases in ChAT activities and loss of cholinergic neurons, linked with decay of cholinergic neurotransmitter functions (Fig. 2) [2, 3]. Also, in cultured differentiated septal cholinergic SN56 cells exogenous Aβ, in pathophysiologically relevant concentrations (0.25–1.0 μmol/L), inhibited pyruvate utilization and acetyl-CoA formation thereby suppressing their viability and ChAT activity as well as ACh content and quantal release [14, 43]. Moreover, other concomitant cytotoxic signals could aggravate these detrimental effects [13, 42, 43]. Alterations of both cholinergic markers correlated significantly with changes in cytoplasmic levels of acetyl-CoA (Fig. 3A, B) [13]. On the other hand, microglial or nondifferentiated neuronal cells appeared to be relatively resistant to such conditions, being compatible with the activation of pyruvate utilization and maintenance fixed acetyl-CoA level in Tg2576 whole brain mitochondria (Fig. 4) [43, 62].

The presented data suggest that in Tg2576 brains accumulation of Aβ alone may bring about Ca^{2+}-dependent non inactivating-indirect inhibition of PDHC activity, yielding acetyl-CoA deficits in both mitochondrial and cytoplasmic compartments of neuronal terminals (Fig. 3A) [46, 52, 53]. Cholinergic neurons are preferentially affected in human AD brain [3], but they seem to be well preserved in Tg2576 model, despite primary disturbances in acetyl-CoA metabolism yielding inhibition of ACh storage and release, without loss of cholinergic neurons as evidenced by unchanged ChAT activity (Figs. 2F, 3B). That raises the supposition that in humans, combination of Aβ with other neurotoxic signals is required for development of complete cholino-destructive AD phenotype [3, 61]. This study indicates that indirect inhibition of PDHC by Aβ may be a very early, yet reversible malfunction suppressing cholinergic transmission due to limited provision of acetyl-CoA in nerve terminals.

ACKNOWLEDGMENTS

This work was supported by Medical University of Gdańsk St57, MN058 and MN059 projects.

Authors' disclosures available online (http://j-alz.com/manuscript-disclosures/15-0327r1).

REFERENCES

[1] Bateman RJ, Xiong C, Benzinger TLS, Fagan AM, Goate A, Fox NC, Marcus DS, Cairns NJ, Xie X, Blazey TM, Holtzman DM, Santacruz A, Buckels V, Oliver A, Moulder K, Aisen PS, Ghetti B, Klunk WE, McDade E, Martins RN, Masters CL, Mayeux R, Ringman JM, Rossor MN, Schofield PR, Sperling RA, Salloway S, Morris JC (2012) Clinical and Biomarker changes in dominantly inherited Alzheimer's disease. *New Engl J Med* **367**, 795-804.

[2] Ikonomovic MD, Klunk WE, Abrahamson EE, Wuu J, Mathis CA, Scheff SW, Myfson EJ, DeKosky ST (2011) Precuneus amyloid burden is associated with reduced cholinergic activity in Alzheimer's disease. *Neurology* **77**, 39-47.

[3] Mufson EJ, Counts SE, Perez SE, Ginsberg SD (2008) Cholinergic system during progression of Alzheimer's disease: Therapeutic implications. *Expert Rev Neurother* **8**, 1703-1718.

[4] Parent MJ, Bedard MA, Aliaga A, Minuzzi L, Mechawar N, Soucy JP, Schirrmacher E, Kostikov A, Gauthier SG, Rosa-Neto P (2013) Cholinergic depletion in Alzheimer's disease shown by [^{18}F]FEOBV autoriadiography. *Int J Molec Imaging* **2013**, 205045.

[5] DeKosky ST, Ikonomovic MD, Styren SD, Beckett L, Wisniewski S, Bennett D, Cochran EJ, Kordower JH, Mufson EJ (2002) Upregulation of choline acetyltransferase activity in hippocampus and frontal cortex of elderly subjects with mild cognitive impairment. *Ann Neurol* **51**, 145-155.

[6] Doraiswamy PM, Sperling RA, Johnson K, Reiman EM, Wong TZ, Sabbagh MN, Sadowsky CH, Fleisher AS, Carpenter A, Joshi AD, Lu M, Grundman M, Mintun MA, Skovronsky DM, Pontecorvo MJ (2014) Florbetapir F^{18} amyloid PET and 36-month cognitive decline: A prospective multicenter study. *Mol Psychiatry* **19**, 1044-1051.

[7] Oddo S, Caccarno A, Sheperd JD, Myrphy MP, Golde TE, Kayed R, Matherrate R, Mattson MP, Akbari Y, LaFerla FM (2003) Triple-transgenic model of Alzheimer's disease with plaques and tangles: Intracellular Aβ and synaptic dysfunction. *Neuron* **39**, 409-421.

[8] Oakley H, Cole SL, Logan S, Maus E, Shao P, Craft J, Guillozet-Bongaarts A, Ohno M, Disterhoft J, Van Eldik L, Berry R, Vassar R (2006) Intraneuronal β-amyloid aggregates, neurodegeneration, and neuron loss in transgenic mice with five familial Alzheimer's disease mutations: Potential factors in amyloid plaque formation. *Neurobiol Dis* **26**, 10129-10140.

[9] Iulita MF, Allard S, Richter L, Munter LM, Ducatenzeiler A, Weise C, Do Carmo S, Klein WL, Multhaup G, Cuello AC (2014) Intracellular Aβ pathology and early cognitive impairments in transgenic rat overexpressing human amyloid precursor protein: A multidimensional study. *Acta Neuropathol Commun* **2**, 61.

[10] Pinho CM, Teixeira PF, Glaser E (2014) Mitochondrial import and degradation of amyloid-β peptide. *Biochim Biophys Acta* **1837**, 1069-1074.

[11] Bubber P, Haroutunian V, Fisch G, Blass JP, Gibson GE (2005) Mitochondrial abnormalities in Alzheimer's brain: Mechanistic implications. *Ann Neurol* **57**, 695-703.

[12] Chen Z, Zhong C (2013) Decoding Alzheimer's disease from perturbed cerebral glucose metabolism: Implications for diagnostic and therapeutic strategies. *Progr Neurobiol* **108**, 21-43.

[13] Szutowicz A, Bielarczyk H, Jankowska-Kulawy A, Pawelczyk T, Ronowska A (2013) Acetyl-CoA the key factor for survival or death of cholinergic neurons in course of neurodegenerative diseases. *Neurochem Res* **38**, 1523-1542.

[14] Bielarczyk H, Jankowska-Kulawy A, Gul S, Pawelczyk T, Szutowicz A (2005) Phenotype dependent differential effects of interleukin-1-β and amyloid-β on viability and cholinergic phenotype of T17 neuroblastoma cells. *Neurochem Int* **47**, 466-473.

[15] Sheu KFR, Kim YT, Blas JP, Weksler ME (1985) An immunochemical study of the pyruvate dehydrogenase deficit in Alzheimer's disease brain. *Ann Neurol* **17**, 444-449.

[16] Morais VA, DeStrooper B (2010) Mitochondrial dysfunction and neurodegenerative disorders: Cause or consequence. *J Alzheimers Dis* **20**(Suppl 2), S255-S263.

[17] Webster SJ, Bachstetter AD, Nelson PT, Schmitt FA, Van Eldik LJ (2014) Using mice to model Alzheimer's dementia: An overview of the clinical disease and the preclinical behavioral changes in 10 mouse models. *Front Genetics* **5**, 88.

[18] Lee JE, Han PL (2013) An update of animal models of Alzheimer's disease with reevaluation of plaque deposition. *Exp Neurobiol* **22**, 84-95.

[19] Schilling S, Zeitschel U, Hoffmann T, Heiser U, Francke M, Kehlen A, Holzer M, Hutter-Paier B, Prokesch M, Windisch M, Jagla W, Schlenzig D, Linder C, Rudolph T, Reuter G, Cynis H, Montag D, Demuth HU, Rossner S (2008) Glutaminyl cyclase inhibition attenuates pyroglutamate Aβ and Alzheimer,s disease-like pathology. *Nat Med* **14**, 1106-1111.

[20] Hartmann J, Kiewert C, Klein J (2010) Neurotransmitters and energy metabolites in amyloid-bearing APP_{SWE}xPSEN1dE9 mouse brain. *J Pharmacol Exp Ther* **332**, 364-370.

[21] Laursen B, Mork A, Plath N, Kristiansen U, Bastlund JF (2014) Impaired hippocampal acetylcholine release parallels spatial memory deficits in Tg2576 mice subjected to basal forebrain cholinergic degeneration. *Brain Res* **1543**, 253-262.

[22] Choi SW, Gerencser AA, Ng R, Flynn JM, Melov S, Danielson SR, Gibson BW, Nicholls DG, Bredesen DE, Brand MD (2012) No consistent bioenergetics defects in presynaptic nerve terminals isolated from mouse models of Alzheimer's disease. *J Neurosci* **32**, 16775-16784.

[23] Yao J, Irwin RW, Zhao L, Nilsen J, Hamilton RT, Brinton RD (2009) Mitochondrial bioenergetics deficit precedes Alzheimer's pathology in female mouse model of Alzheimer's disease. *Proceed Natl Acad Sci U S A* **106**, 14670-14675.

[24] Szutowicz A, Bielarczyk H, Gul S, Ronowska A, Pawelczyk T, Jankowska-Kulawy A (2006) Phenotype-dependent susceptibility of cholinergic neuroblastoma cells to neurotoxic inputs. *Dev Neurosci* **21**, 149-161.

[25] Bielarczyk H, Szutowicz A (1989) Evidence for regulatory function of synaptoplasmic acetyl-CoA in acetylcholine synthesis in nerve endings. *Biochem J* **262**, 377-380.

[26] Tuček S (1993) Short-term control of the synthesis of acetylcholine. *Prog Biophys Molec Biol* **60**, 59-69.

[27] Szutowicz A, Bielarczyk H (1987) Elimination of CoASH interference from acetyl-CoA assay by maleic anhydride. *Anal Biochem* **164**, 292-296.

[28] Israel M, Lesbats B (1982) Application to mammalian tissues of the chemiluminescent method for detecting acetylcholine. *J Neurochem* **39**, 250-348.

[29] Fonnum F (1975) A rapid radiochemical method for the determination of choline acetyltransferase. *J Neurochem* **24**, 407-409.

[30] Szutowicz A, Stępień M, Piec G (1981) Determination of pyruvate dehydrogenase and acetyl-CoA synthetase activities using citrate synthase. *Anal Biochem* **115**, 81-87.

[31] Pawełczyk T, Angielski S (1984) Cooperation of Ca and pH in regulation of the activity of the 2-oxoglutarate dehydrogenase complex and its components from bovine kidney cortex. *Acta Biochim Pol* **3**, 289-305.

[32] De Villafranca GW, Haines VE (1974) Paramyosin from arthropod cross-striated muscle. *Comp Biochem Physiol B* **47**, 9-26.

[33] Plaut GW, Aogaichi T (1968) Purification and properties of diphosphopyridine nuleotide-linked isocitrate dehydrogenase of mammalian liver. *J Biol Chem* **243**, 5572-5583.

[34] Szutowicz A, Angielski S (1970) Regulation of ATP citrate lyase activity *in vitro*. *Acta Biochim Pol* **17**, 159-174.

[35] Ryan DA, Narrow WC, Federoff HJ, Bowers WJ (2010) An improved method for generating consistent soluble amyloid-beta oligomer preparations for *in vitro* neurotoxicity studies. *J Neurosci Meth* **190**, 171-179.

[36] Bradford M (1976) A rapid sensitive method for the quantitation of microgram quantities of protein utilizing the principle of protein-dye binding. *Anal Biochem* **72**, 248-254.

[37] Apelt J, Kumar A, Schliebs R (2002) Impairment of cholinergic neurotransmission in adult and aged transfenic Tg2576 mouse brain expressing Swedish mutation of human β-amyloid precursor protein. *Brain Res* **953**, 17-30.

[38] DeMattos RB, Lu J, Tang Y, Racke MM, DeLong CA, Tzaferis JA, Hole JT, Forster BM, McDonnel PC, Liu F, Kinley RD, Jordan WH, Hutton ML (2012) A plaque-specific antibody clears existing β-amyloid plaques in Alzheimer's disease mice. *Neuron* **76**, 908-920.

[39] Miners JS, Jones R, Love S (2014) Differential changes in Aβ42 and Aβ40 with age. *J Alzheimers Dis* **40**, 727-735.

[40] Zheng Y, Zhang J, Zhu Y, Zhang J, Shen H, Lu J, Pan X, Lin N, Dai X, Zhou M, Chen X (2015) Tripchlorolide improves cognitive deficits by reducing amyloid β and upregulating synapse-related proteins in transgenic model of Alzheimer's Disease. *J Neurochem* **133**, 38-52.

[41] Mitani Y, Yarimizu J, Akashiba H, Shitaka Y, Ni K, Matsuoka N (2013) Amelioration of cognitive deficits in plaque-bearing Alzheimer's disease model mice through selective reduction of nascent soluble Aβ42 without affecting Aβ pools. *J Neurochem* **125**, 465-472.

[42] Bielarczyk H, Gul S, Ronowska A, Bizon-Zygmańska D, Pawelczyk T, Szutowicz A (2006) RS-α-lipoic acid protects cholinergic cells against sodium nitroprusside and amyloid-β neurotoxicity through restoration of acetyl-CoA level. *J Neurochem* **98**, 1242-1251.

[43] Bielarczyk H, Jankowska A, Madziar B, Matecki A, Michno A, Szutowicz A (2003) Differential toxicity of nitric oxide,

aluminium and amyloid β peptide in SN56 cholinergic cells from mouse septum. *Neurochem Int* **42**, 323-331.

[44] Hoshi M, Takashima A, Murayama M (1997) Nontoxic amyloid-β-peptide1-42 suppresses acetylcholine synthesis. *J Biol Chem* **272**, 2038-2041.

[45] Hoshi M, Takashima A, Noguchi K, Murayama M, Sato M, Kondo S, Saitoh Y, Ishiguro K, Hoshino T, Imahori K (1996) Regulation of mitochondrial pyruvate dehydrogenase activity by tau protein kinase I/glycogen synthase kinase 3β in brain. *Proc Natl Acad Sci U S A* **93**, 2719-2723.

[46] Del Prete D, Checler F, Chami M (2014) Ryanodine receptors: Physiological function and dysregulation in Alzheimer's disease. *Mol Neurodegener* **9**, 21.

[47] Du H, Guo L, Yan S, Sosunov AA, McKhann GM, Yan SSD (2010) Early deficits in synaptic mitochondria in Alzheimer's disease mouse model. *Proc Natl Acad Sci U S A* **107**, 18670-18675.

[48] Steinert JR, Chernova T, Forsythe ID (2010) Nitric oxide signaling in brain function, dysfunction and dementia. *Neuroscientist* **16**, 435-452.

[49] Krištofiková Z, Kozmiková I, Hovorková P, Řičny J, Zach P, Majer E, Klaschka J, Řipová D (2008) Lateralization of hippocampal nitric oxide mediator system in people with Alzheimer disease, multi-infarct dementia and schizophrenia. *Neurochem Int* **52**, 118-125.

[50] Subash S, Essa MM, Al-Asmi A, Al-dawi S, Vaishnav R, Braidy N, Manivasagam T, Guillemin GJ (2014) Pomegranate from Oman alleviates the brain oxidative damage in transgenic mouse model of Alzheimer's disease. *J Tradit Complement Med* **4**, 232-238.

[51] Lalande J, Halley H, Balayssac S, Gilard V, Dejean S, Martino R, Frances B, Lassale JM, Malet-Martino M (2014) ^{1H} NMR metabolomics signatures in five brain regions of the AβPPswe Tg2576 mouse model of Alzheimer's disease at four ages. *J Alzheimers Dis* **39**, 121-143.

[52] WangY, Mattson MP (2014) L-type Ca^{2+} currents at CA1 synapses, byt not CA3 or dentate granule neuron synapses, are increased in 3xTgAD mice in an age-dependent manner. *Neurobiol Aging* **35**, 88-95.

[53] Hardas SS, Sultana R, Clark AM, Beckett TL, Szweda LI, Murphy MP, Butterfield DA (2013) Oxidativemodification of lipoic acid by HNE in Alzheimer disease brain. *Redox Biol* **1**, 80-83.

[54] Sancheti H, Kanamori K, Patil I, Diaz Brinton R, Ross BD, Cadenas E (2014) Reversal of metabolic deficits by lipoic acid in triple transgenic mouse model of Alzheimer's disease: A 13C NMR study. *J Cereb Blood Flow Metab* **34**, 288-296.

[55] Gibson GE, Chen HL, Xu H, Qiu L, Xu Z, Denton TT, Shi Q (2012) Deficits in the mitochondrial enzyme α-ketoglutarate dehydrogenase lead to Alzheimer's disease-like calcium dysregulation. *Neurobiol Ageing* **33**, 1121. e13-1121.e24.

[56] Craddock TJA, Tuszyński JA, Chopra D, Casey N, Goldstein LE, Hameroff SR, Tanzi RE (2012) The Zinc dyshomeostasis hypothesis of Alzheimer's disease. *Plos One* **7**, e33552.

[57] Sensi SL, Paoletti P, Bush AI, Sekler I (2009) Zinc in the physiology and pathology of the CNS. *Nat Rev Neurosci* **10**, 780-792.

[58] Ronowska A, Dyś A, Jankowska-Kulawy A, Klimaszewska-Łata J, Bielarczyk H, Romianowski P, Pawelczyk T, Szutowicz A (2010) Short-term effects of zinc on acetylcholine metabolism and viability of SN56 cholinergic neuroblastoma cells. *Neurochem Int* **56**, 143-151.

[59] Tortora V, Quijano C, Freeman B, Radi R, Castro L (2007) Mitochondrial aconitase reaction with nitric axide, S-nitrosoglutathione, and peroxynitrite: Mechanisms and relative contribution to aconitase inactivation. *Free Radic Biol Med* **42**, 1075-1088.

[60] Lee JY, Cho E, Seo JW, Hwang JJ, Koh JY (2012) Alternation of the cerebral zinc pool in a mouse model of Alzheimer disease. *J Neuropathol Exp Neurol* **71**, 211-222.

[61] Korczyn AD (2012) Why have we failed to cure Alzheimer's disease? *J Alzheimers Dis* **29**, 275-282.

[62] Klimaszewska-Łata J, Gul-Hinc S, Bielarczyk H, Ronowska A, Zyśk M, Grużewska K, Pawelczyk T, Szutowicz A (2015) Differential effects of lipopolysaccharide on energy metabolism in murine microglial N9 and cholinergic SN56 neuronal cells. *J Neurochem* **133**, 284-297.